# Supporting Information

## CompassR-guided recombination unlocks design principles to stabilize a lipase in ILs with minimal experimental efforts

*Haiyang Cui[1,2], Subrata Pramanik[1], Karl-Erich Jaeger[3,4], Mehdi D. Davari[1*], Ulrich Schwaneberg[1,2*]*

[1]Institute of Biotechnology, RWTH Aachen University, Worringerweg 3, Aachen 52074, Germany

[2]DWI-Leibniz Institute for Interactive Materials, Forckenbeckstraße 50, Aachen 52056, Germany

[3]Institute of Molecular Enzyme Technology, Heinrich Heine University Düsseldorf, Wilhelm Johnen Strasse, Jülich, Germany

[4]Institute of Bio-and Geosciences IBG 1: Biotechnology, Forschungszentrum Jülich GmbH, Wilhelm Johnen Strasse Jülich, Germany

# Table of contents

## Activity profile in buffer and ILs of improved BSLA variants

In addition, the purified variant M1a, M1b, and M1c were studied more closely by investigating the specific activtiy at 40 %(v/v) [BMIM]Cl, 10 %(v/v) [BMIM]I, 80 %(v/v) [BMIM]Br, and 30 %(v/v) [BMIM][TfO] (**Figure S2**). BSLA WT was also examined for comparetion. The specific activtiy for BSLA WT in **Figure S2** closely match those reported values [1]. As expected, the specific activity of BSLA WT was reduced from 11.5 U/mg in buffer to 4.3 U/mg, 7.8 U/mg, 2 U/mg, and 4.7 U/mg toward 40 %(v/v) [BMIM]Cl, 10 %(v/v) [BMIM]I, 80 %(v/v) [BMIM]Br, and 30 %(v/v) [BMIM][TfO], respectively. All three variants showed notably improved specific activity in buffer (M1a: 2.2-fold, M1b: 1.9-fold, M1c: 2.1-fold). Significant improvement of specific activity of all three variants were also observed in presence of [BMIM]Cl, [BMIM]I, and [BMIM]Br with ranging from 1.1-fold to 2.5-fold. In contrast with [BMIM]-halogen ILs, M1a, M1b, and M1c had decread specific activtiy in 30 %(v/v) [BMIM][TfO], which indicating the molecular mechanisms of deactivating enzyme in ILs with different anion might not be the consistent [2].

## Overall conformational change of BSLA variants in ILs

It was observed that all simulations converged after ~60 ns yielding final RMSD values of ~1.5-2.5 Å. Analysis of RMSDs showed that RMSD of BSLA WT was retained within ~1.5-2.3 Å in four ILs. Both variants showed RMSDs within ~1.5 - 2.5 Å in all ILs (Supplementary **Figure S3**). These observations indicate that the structures of BSLA WT and variants remain stable in binary mixtures of ILs and water at experimental concentrations (i.e., 40 %(v/v) [BMIM]Cl, 10 %(v/v) [BMIM]I, 80 %(v/v) [BMIM]Br, and 30 %(v/v) [BMIM][TfO]). In [BMIM]-halogen ILs, RMSD of backbone atoms reveal that the conformational mobility of both variants was almost similar even more stable in comparison to BSLA WT. The corresponding results were also shown in the results of RMSF, $R_g$, and total SASA, which show no significant change (Supplementary **Figure S4-5**). This observation is also consistent with our previous report, in which we have revealed that the structure of BSLA was stable in ILs (concentrations ~10-19% v/v) [2]. However, the RMSD of variants slightly increased in [BMIM][TfO], suggesting both variants exert partial dynamics of the overall structures compared with BSLA WT. According to the activity results, this slightly destabilized structure of variants might be another reason for the reducing activity in [BMIM][TfO], besides the anion TfO- solvation change (**Figure 5**). Moreover, the RMSF of variants and WT have an almost

different feature comparing to in three [BMIM]-halogen ILs. In a recreant report, it has been suggested that enzyme flexibility is correlated to the hydration of enzyme [3]. These results also indicate that the molecular mechanism of BSLA-IL interaction might be distinct between [BMIM]-halogen ILs and [BMIM][TfO].


**Solvation phenomenon of cations and anions**

It was observed that BMIM$^+$ cations remain dominant in surface interactions of BSLA WT and variants in the case of [BMIM]Cl, [BMIM]Br, and [BMIM]I (**Figures 5a, 5c,** and **5e**). WT and both variants M1a and M1c remain similar number of BMIM$^+$ in [BMIM]Cl, [BMIM]Br, and [BMIM]I. Moreover, anions remained mostly in the bulk of water (**Figure S7**). This observation led to the conclusion that the reduction of BSLA WT activity is attributed to the surface interactions of BMIM$^+$ cations, which resulting in tripping off essential water molecules from the BSLA surface. However, a critical phenomenon was observed in the case of [BMIM][TfO], in which cations and anions interact equally (**Figures 5a** and **S7**). Surface interactions of TfO$^-$ might be a critical factor along with BMIM$^+$ interactions to decrease specific activity in [BMIM][TfO]. According to specific activity data, BSLA WT and variants showed lower activity in [BMIM][TfO] than the buffer. However, both variants showed reduced activity compared to BSLA WT in [BMIM][TfO]. This observation indicates that TfO$^-$ anions might have a beneficial effect on BSLA activity. To understand this, we analyzed the number of TfO$^-$ anions on the surface of BSLA WT and both variants, and we found that a higher number of TfO$^-$ anions interact on the BSLA WT surface when compared with both variants (**Figures 5a** and **S5**). A similar observation was shown in BMIM$^+$ (**Figure 5c**).


**The structural change and solvation phenomenon in the active site**

For the active site of BSLA variants and WT in the same IL, there is no significant and/or frequent change in terms of the flexibility of catalytic triad (Ser77, Asp133, and His156) and oxyanion hole (Ile12 and Met78) regarding their RMSF value (**Figure S4,** black asterisks). However, the flexibility of active site in [BMIM][TfO] showed significantly decreased feature comparing to in three [BMIM]-halogen ILs, which agrees well with the change of overall structure. To examine how the water or IL molecule behaves in the substrate binding cleft of BSLA WT and variants, the average number of water and BMIM$^+$ and anion were calculated based on the last 40 ns of the MD trajectories, and the results are shown in **Figure S8**. As the

previous study suggested, BSLA active site was defined as the region which expands 5.9 Å away from the Ser77 residue located at the bottom of the BSLA active site [4]. In water system, the number of water towards BSLA M1a and M1b was decreased from ~7 to ~5 compared to WT. However, in IL [BMIM]Cl, the active site of M1a and M1b were well hydrated with ~7 water molecules when compared to BSLA WT (**Figure S8a**). However, this phenomenon is not shown in other ILs. Similar results are observed for BMIM⁺ and four anions as well (**Figure S8b** and **S8c**). Interestingly, there is no TfO⁻ anion in the active site in all three BSLA variants (**Figure S8c**).

**Table S1.** Primers used for iterative site-directed mutagenesis studies. The mutated codon is underlined.

| Name | 5 --> 3 sequence |
| --- | --- |
| A81M Forward Primer | GGGGGGC<u>ATG</u>AACACACTT |
| A81M Reverse Primer | AAGTGTGTT<u>CAT</u>GCCCCCC |
| V165L Forward Primer | GCAGCCA<u>TTT</u>AACAGCCTG |
| V165L Reverse Primer | CAGGCTGTT<u>AAA</u>TTGGCTGC |
| G155 Forward Primer | CATGGCGTT<u>NNK</u>CACATCGGCC |
| G155 Reverse Primer | GGCCGATGT<u>MNN</u>GAACGCCATG |

**Table S2.** Analysis of BSLA amino acid conservation on identified amino acid positions[a]

| Position | BSLA amino acid | Score | Residue variety |
|---|---|---|---|
| 5 | P | 9 | P, A |
| 36 | L | 8 | R, T, L, A, P, V, M, F |
| 46 | G | 4 | M, D, V, E, Q, G, Y, A, K, T, R |
| 81 | A | 6 | V,M,S,I,N,T,L,Y,A |
| 104 | T | 6 | T, S, A, G |
| 114 | L | 4 | D, I, V, L, P, T, A |
| 129 | Y | 6 | T, P, Y, S |
| 155 | G | 1 | A,S,T,G,D |
| 165 | V | 9 | V |

[a] Residue conservation calculated by ConSurf-DB [5] with the following parameters: BSLA structure PDB: 1i6w, Chain A; Multiple Sequence Alignment was built using MAFFT; the Homologues were collected from UNIREF90; homolog search algorithm: HMMER; HMMER E-value: 0.0001; No. of HMMER iterations: 1; maximal 95 % ID between sequences; minimal 35 % ID For homologs; 150 sequences that sample the list of homologues to the query. The number scale representing the conservation scores (9 - conserved, 1 - variable).

**Table S3.** The normalized activity of the identified BSLA recombinants

| Library[a] | The active ratio of SSM library[a] | Variant | Substitutions[b] | Normalized activity in buffer[c,d] |
|---|---|---|---|---|
| | | WT | - | 1.0 ± 0.03 |
| A | 77.8 % | M1 | F17S/V54K/D64N/D91E[6] | 1.0 ± 0.06 |
| | | M1a | F17S/V54K/D64N/D91E/<u>G155N</u> | 1.6 ± 0.13 |
| | | M1b | F17S/V54K/D64N/D91E/<u>G155S</u> | 0.6 ± 0.04 |
| | | M1c | F17S/V54K/D64N/D91E/<u>G155D</u> | 3.5 ± 0.14 |
| B | 51.1 % | M2 | F17S/V54K/D64N/D91E/<u>A81M</u> | 0.2 ± 0.06 |
| C | 37.0 % | M3 | F17S/V54K/D64N/D91E/<u>V165L</u> | 0.2 ± 0.07 |

[a]Variant M1, M2, and M3 were as the parent for SSM library A, B, and C generation at amino acid position 155, respectively. Residual activity (in buffer) is between 0 - 10 % of the BSLA wild type activity and are referred to as "inactive" recombinant. The active ratio is calculated with 90 clones from each SSM library.

[b]In order to comparing to the starting variant M1 from previous work [6], the new recombined substitution(s) was marked with an underline.

[c]Normalized activity of the BSLA supernatant was calculated according to the number of cells measured by $OD_{600}$ and was relative to BSLA WT.

[d]All data shown are average values from measurements in triplicates or more.

**Table S4.** Performance comparison between the current work with other (semi-)rational design approaches for improving the enzymatic properties by recombination.

| Method | Screening effort | | Library quality | |
|---|---|---|---|---|
| | Theoretical library size | Total number of screened clones | Fraction of active recombinant | Chance to find improved variant[a] |
| Current work | 59 | 272 | 37.0-77.8 % | 2 % |
| TtL rational design[b,7] | 8 | 8 | - | 0 |
| Loop engineering [8] | 4096 | 2000 | - | 0.3 % |
| PELE-guided [9] | 400 | 1500 | - | 0.2 % |
| SCHEMA-RASPP[10] | >81 | 1000 | - | 1.4 % |
| CASTing [c,11] | 40 | 360 | 0 | 0 |
| OmniChange[11] | $20^4$ | 3500 | 1.2 % | 0.05 % |
| Reshaping binding pocket[12] | 1028 | 3320 | 16.7 % | 0.2 % |

[a]The number of improved variants is divided by the number of screened variants.

[b]The mutations were chosen based on several approaches aimed at improving enzyme activity and stability in ILs.

[c]Only the data in path I and II in literature[11] were shown.
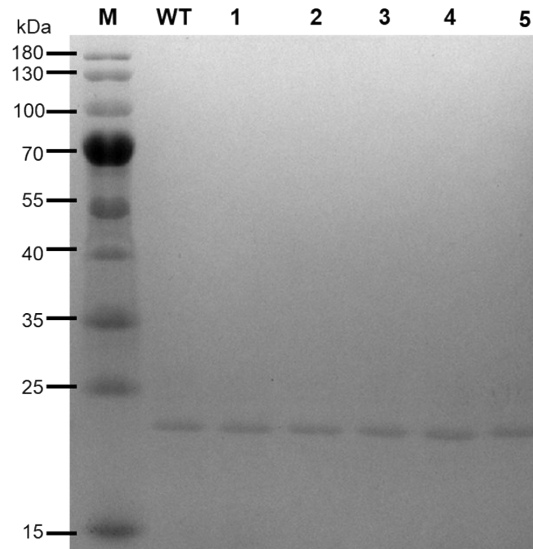
**Figure S1.** Identification and SDS-PAGE analysis of the purified BSLA protein. The purified protein was loaded onto 5 % stacking gel and 12 % separating gel. A wide molecular weight standard protein (15-180 kDa) acts as marker, the remaining five lanes is the same sample volume of WT: wild type; M1a: F17S/V54K/D64N/D91E/G155N; M1b: F17S/V54K/D64N/D91E/G155S; M1c: F17S/V54K/D64N/D91E/G155D; M2: F17S/V54K/D64N/D91E/A81M; M3: F17S/V54K/D64N/D91E/V165L, respectively, from left to right. The gel was stained with Coomassie Brilliant Blue.
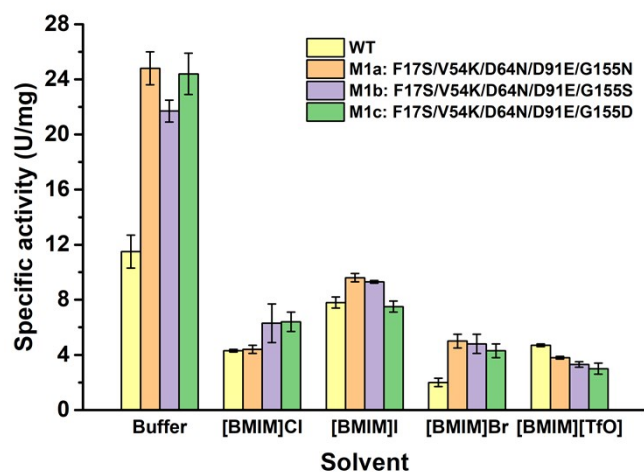
**Figure S2.** The specific activity of purified BSLA WT and selected recombinants in the buffer and four ILs cosolvent. Specific activity was measured directly in TEA buffer or ILs at room temperature. The concentration of [BMIM]Cl, [BMIM]I, [BMIM]Br, [BMIM][TfO] cosolvent is 40 %(v/v), 10 %(v/v), 80 %(v/v), and 30 %(v/v), respectively. All data shown are average values from measurements in triplicates or more.
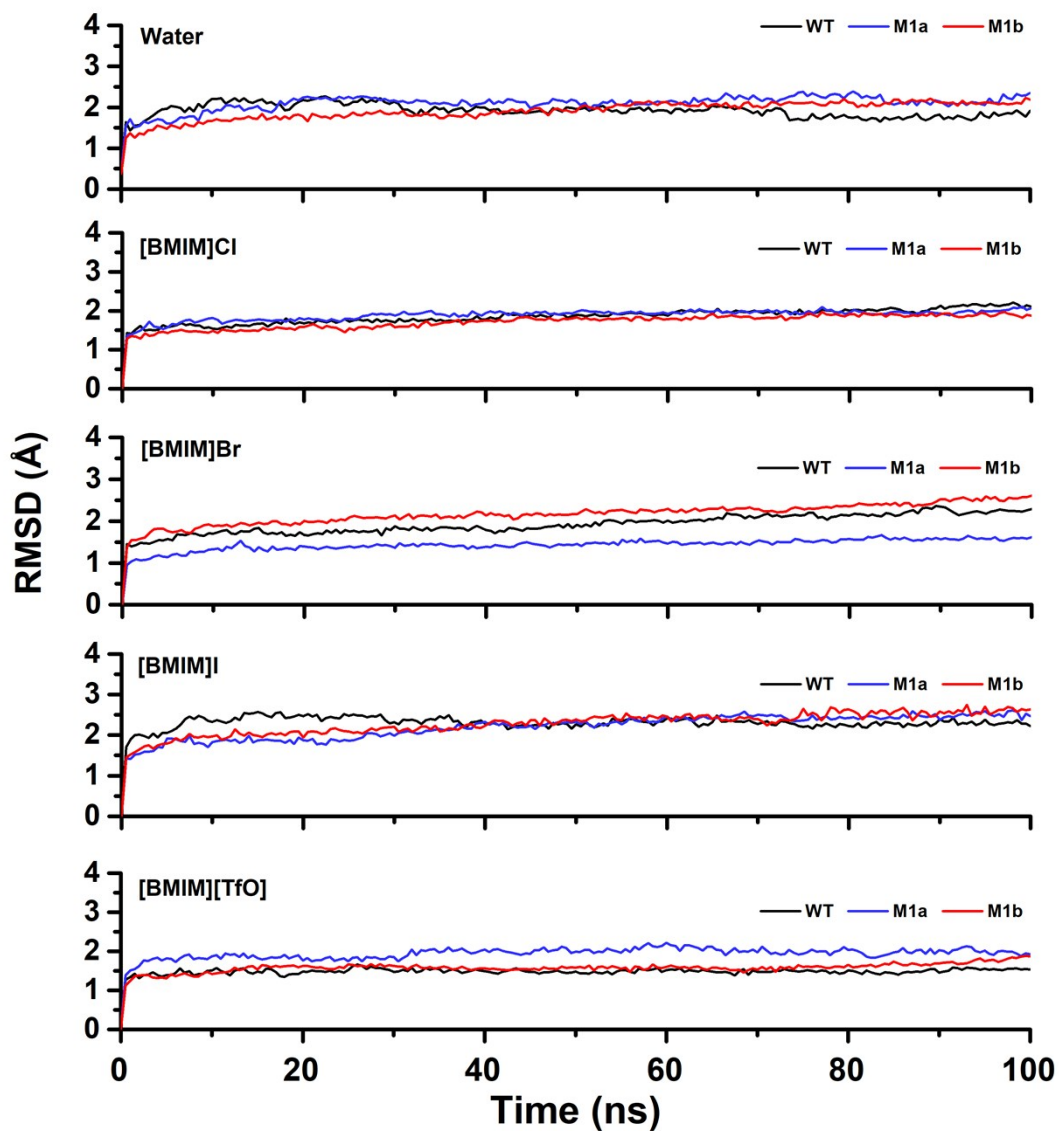
**Figure S3.** Root-mean-square deviation (RMSD) of the BSLA WT, variants M1a and Mb backbone with respect to the initial structure as a function of time in water and ILs [BMIM]Cl (40 % v/v), [BMIM]I (10 % v/v), [BMIM]Br (80 % v/v), and [BMIM][TfO] (30 % v/v). RMSD value is averaged from three MD simulations runs with different starting atomic velocities. WT: wild type. M1a: 17S/V54K/D64N/D91E/G155N. M1b: F17S/V54K/D64N/D91E/G155S.
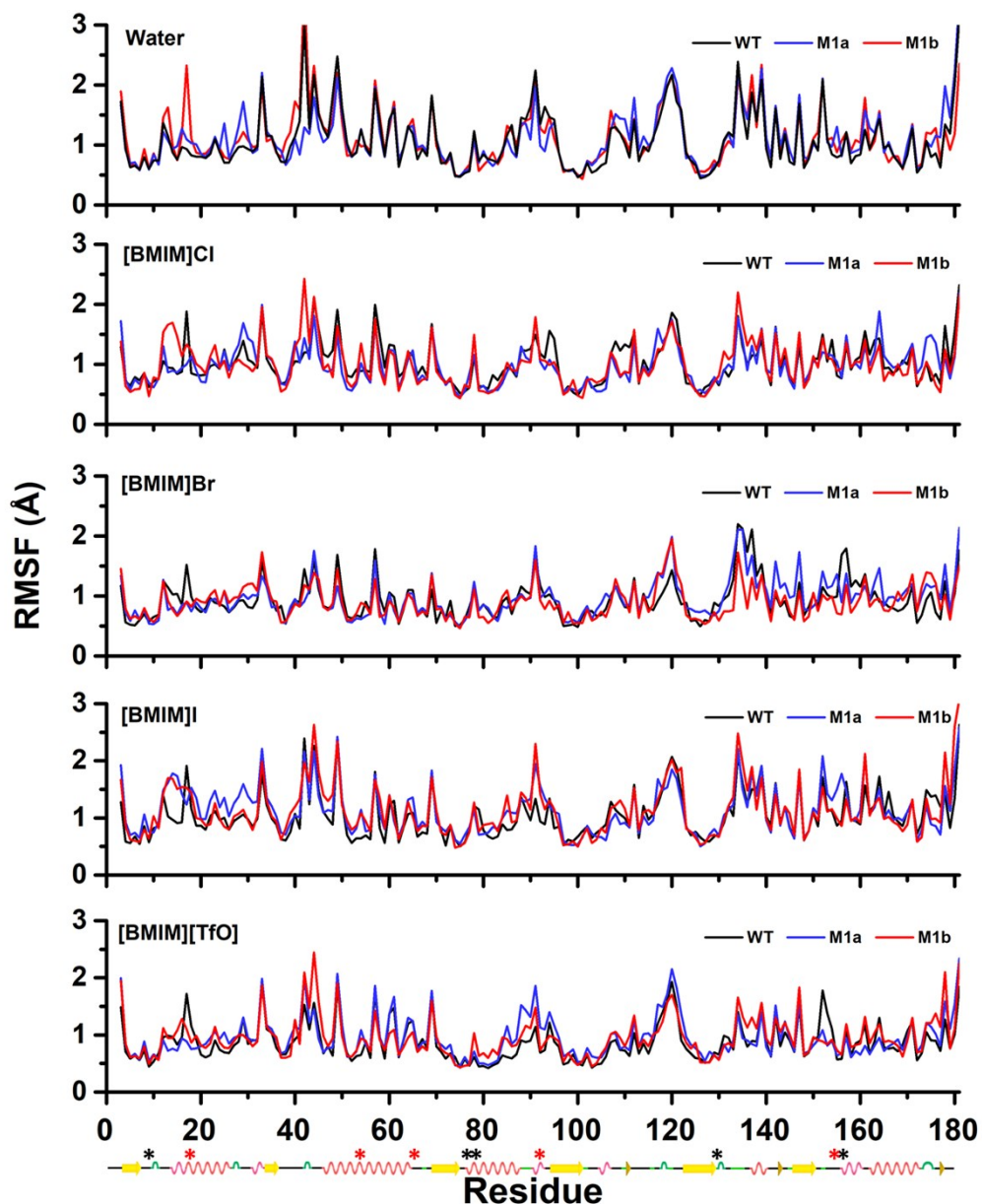
**Figure S4.** Averaged RMSF of each residue determined from the last 40 ns of three independent simulations towards the BSLA WT, M1a and M1b in water and ILs [BMIM]Cl (40 % v/v), [BMIM]I (10 % v/v), [BMIM]Br (80 % v/v), and [BMIM][TfO] (30 % v/v). The secondary structure elements were calculated using the DSSP program [13]. Secondary structure elements are shown as following color schemes: β-sheet (yellow), α-helix (pink), 3/10-helix (red), and turn, β-bridge, and bend (green). Catalytic triad (Ser77, Asp133, and His156) and oxyanion hole (Ile12 and Met78) are labeled with black asterisks. The substitutions of M1a and M1b are labeled with red asterisk. WT: wild type. M1a: 17S/V54K/D64N/D91E/G155N. M1b: F17S/V54K/D64N/D91E/G155S.
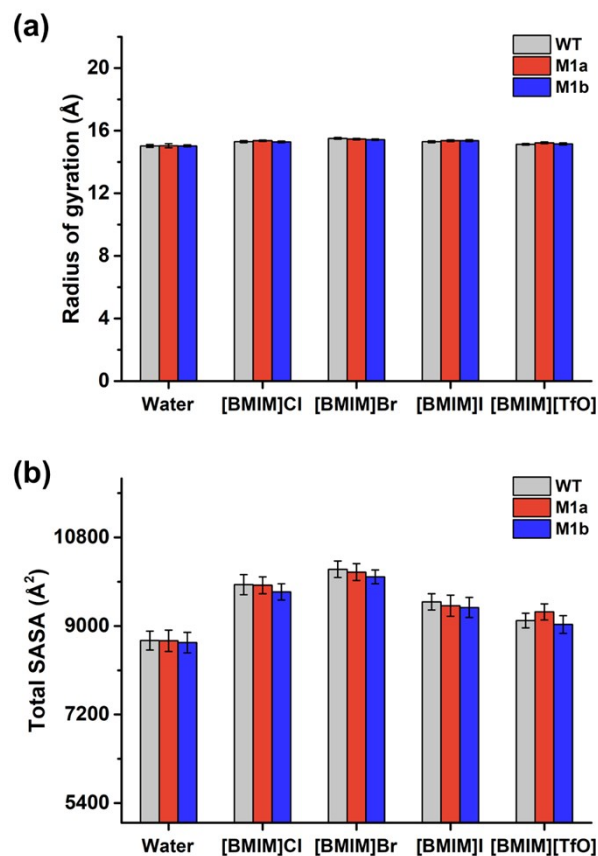
**Figure S5.** Overall conformational change analysis in ILs.(**a**) The radius of gyration ($R_g$) of BSLA WT and variants in ILs [BMIM]Cl (40 % v/v), [BMIM]I (10 % v/v), [BMIM]Br (80 % v/v), and [BMIM][TfO] (30 % v/v). The time-averaged radius of gyration was calculated from the last 40 ns of the simulation. Error bars show the standard deviation from three independent runs for each variant. (**b**) The time-averaged total SASA of the BSLA WT and variants in ILs. The average of SASA of BSLA is computed based on the last 40 ns of each simulation. Here, SASA refers to the surface area of BSLA, which is accessible to water molecules and organic solvents molecules calculated using a probe of radius 1.4 Å.WT: wild type. M1a: 17S/V54K/D64N/D91E/G155N. M1b: F17S/V54K/D64N/D91E/G155S.
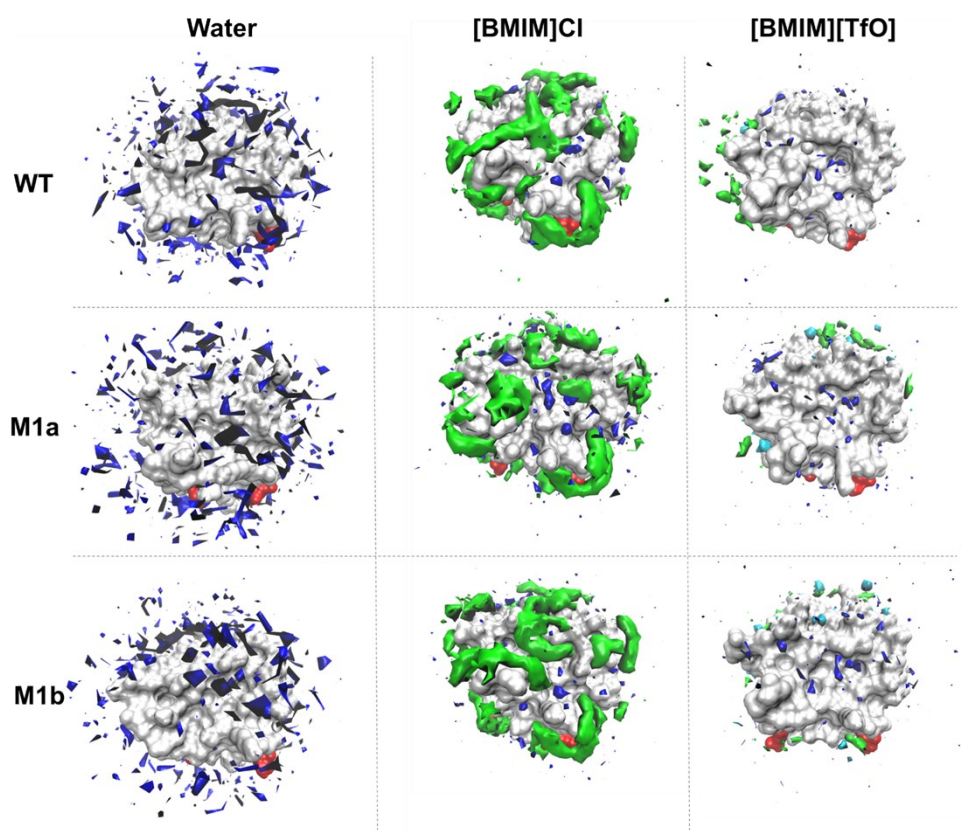
**Figure S6.** Spatial distribution of water and IL molecules at the molecular surface of the BSLA variant in water, [BMIM]Cl and [BMIM][TfO]. The BSLA surface is shown in grey, Ser77, Asp133, His156 (the catalytic triad) in magenta; the cation BMIM$^+$ molecules in green, anion molecules Cl$^-$ , and TfO$^-$ in cyan; the water molecules in blue; and the substitutions in red. The 180° rotation of BSLA is shown in **Figure 5** to give a complete view of the surface. Each view of BSLA has the same orientation. The contours are shown with the isovalue 11 for water, and isovalue 23, 37, 41 for BMIM$^+$, Cl$^-$, TfO$^-$ molecules, respectively in ILs systems. The contours are shown with the isovalue 110 for water in pure water system.
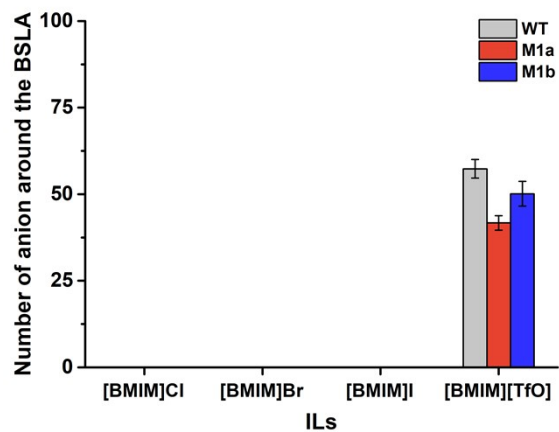
**Figure S7.** The average number of anions interacting within the first solvation shell (~2.25 Å for Cl⁻, Br⁻, and I⁻; ~6.50 Å for TfO⁻ from BSLA surface) of the BSLA WT and variants M1a and M1c. Anion value is averaged in the last 40 ns from three MD simulations runs.
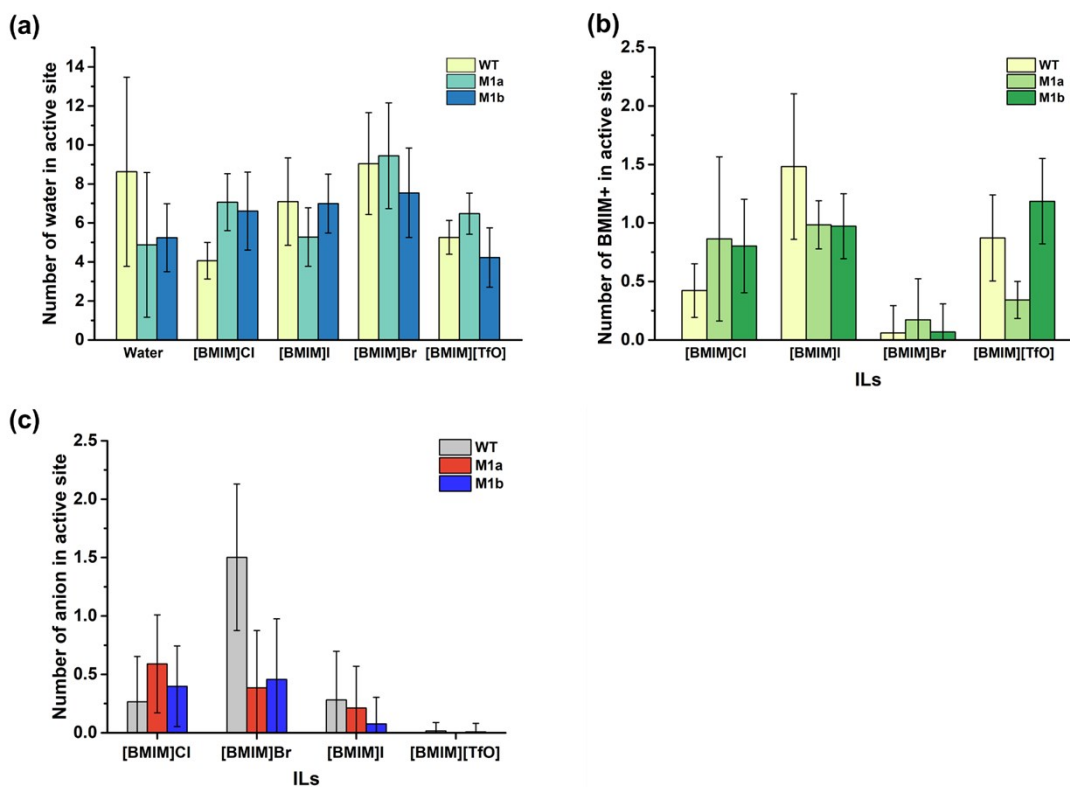
**Figure S8.** Solvation phenomenon in BSLA active site. The average number of (**a**) water, (**b**) BMIM+, and (**c**) anion in the active site of BSLA WT and variants during the MD simulations. The number of the molecule was averaged over the last 40 ns from three independent MD runs. The cutoff 5.9 Å was used to calculate the number of water, IL cation and anion in active site [4].

**References**

1. J. Zhao, N. Jia, K. E. Jaeger, M. Bocola and U. Schwaneberg, *Biotechnol. Bioeng.*, 2015, **112**, 1997-2004.
2. S. Pramanik, G. V. Dhoke, K. E. Jaeger, U. Schwaneberg and M. D. Davari, *ACS Sustain. Chem. Eng.*, 2019.
3. J. N. Dahanayake and K. R. Mitchell-Koch, *Front. Mol. Biosci.*, 2018, **5**, 65.
4. H. Cui, T. H. Stadtmüller, Q. Jiang, K. E. Jaeger, U. Schwaneberg and M. D. Davari, *ChemCatChem*, 2020, **12**, 4073.
5. G. Celniker, G. Nimrod, H. Ashkenazy, F. Glaser, E. Martz, I. Mayrose, T. Pupko and N. Ben-Tal, *Isr. J. Chem.*, 2013, **53**, 199-206.
6. H. Cui, H. Cao, H. Cai, K. E. Jaeger, M. D. Davari and U. Schwaneberg, *Chem. Eur. J*, 2020, **26**, 643-649.
7. J. C. Stevens, D. W. Rodgers, C. Dumon and J. Shi, *Front. Energy Res.*, 2020, **8**.
8. A.-M. Wallraf, H. Liu, L. Zhu, G. Khalfallah, C. Simons, H. Alibiglou, M. D. Davari and U. Schwaneberg, *Green Chem.*, 2018, **20**, 2801-2812.
9. I. Mateljak, E. Monza, M. F. Lucas, V. Guallar, O. Aleksejeva, R. Ludwig, D. Leech, S. Shleev and M. Alcalde, *ACS Catal.*, 2019, **9**, 4561-4572.
10. I. Mateljak, A. Rice, K. Yang, T. Tron and M. Alcalde, *ACS Synth. Biol.*, 2019, **8**, 833-843.
11. Y. Ensari, G. V. Dhoke, M. D. Davari, A. J. Ruff and U. Schwaneberg, *ChemBioChem*, 2018, **19**, 1563-1569.
12. Z. Sun, R. Lonsdale, X.-D. Kong, J.-H. Xu, J. Zhou and M. T. Reetz, *Angew. Chem., Int. Ed.*, 2015, **54**, 12410-12415.
13. W. Kabsch and C. Sander, *Biopolymers*, 1983, **22**, 2577-2637.